s-Process Zirconium in Presolar Silicon Carbide Grains

Günther K. Nicolussi, Andrew M. Davis, Michael J. Pellin, Roy S. Lewis, Robert N. Clayton, Sachiko Amari*

The isotopic composition of zirconium in silicon carbide grains from the Murchison meteorite was measured by resonant ionization mass spectrometry of laser-ablated neutral atoms. These grains are condensates from the atmospheres of red giant stars that existed before the formation of our sun and solar system, and they contain records of nucleosynthesis in these stars. The r-process–dominated isotope zirconium-96 was depleted by more than a factor of 2 compared with the s-process–dominated isotopes zirconium-90, zirconium-91, zirconium-92, and zirconium-94, in agreement with expectations for neutron capture nucleosynthesis in asymptotic giant branch stars.

The presence of relict presolar material in the solar system was hinted at with the discovery of enrichments in the heavy and light isotopes of xenon in meteorites (*1*), it was established with the discovery of ^{22}Ne enrichments in meteorites in 1972 (*2*), and it has been widely accepted since the discovery in 1972 of ^{16}O-rich materials in meteorites (*3*), but the discoveries of the identities of the presolar grains did not begin until 1987 (*4*). Five presolar phases have been identified in carbonaceous and unequilibrated ordinary chondrites: diamond (mean size 2.6 nm) (*4*, *5*), silicon carbide (<0.05 to 20 μm) (*6*, *7*), graphite (0.8 to 7 μm) (*8*), aluminum oxide (*9*–*11*), and silicon nitride (*12*). The properties of presolar grains in meteorites have been reviewed (*13*, *14*). The strongest evidence for the presolar origin of these grains is the anomalous isotopic composition of Si, C, N, and O, as measured in individual grains by secondary ion mass spectrometry.

Silicon carbide is the best studied type of presolar grain, because it occurs as relatively large grains and it incorporates a number of minor and trace elements. The majority of SiC grains have nuclear abundances suggesting condensation around low-mass (1 to 3 $M_\odot$, where $M_\odot$ is the mass of the sun), thermally pulsing, asymptotic giant branch (TP-AGB) stars (*15*–*17*). Relative to solar abundances, these grains have enhanced ^{12}C/^{13}C ratios and diminished ^{14}N/^{15}N ratios, and they are enriched in ^{29}Si and ^{30}Si relative to ^{28}Si. Many of them also had high initial ^{26}Al/^{27}Al ratios.

Aggregates of SiC grains show enrichments in the s-process isotopes of heavy elements (*13*, *14*). In the s-process, nucleosynthesis occurs by neutron capture under conditions in which neutron densities are low enough to allow beta decay of short-lived radionuclides before another neutron capture can occur (*18*). Whereas isotope ratios of several light elements (C, N, Mg, Si, Ca, and Ti) have been measured in individual presolar grains (*13*), isotope ratios of some elements beyond the Fe peak, Kr, Sr, Xe, Ba, Nd, Sm, and Dy (*16*, *19*–*24*), have been measured only in aggregates of many grains. Each presolar SiC grain may have come from a different star, and grain-size separated aggregates have shown varying degrees of s-process enrichment for Kr, Sr, and Ba (*16*, *19*–*23*), as well as varying s-process end member compositions. Measurements of the isotopic composition of Si and C in individual SiC grains show large differences from grain to grain, reflecting the unique nucleosynthetic history of each grain. It follows that detailed information on heavy-element nucleosynthesis requires isotopic analysis of single grains.

Our first target element was Zr, for the following reasons: (i) Zr is the most abundant heavy element in most SiC grains (*25*); (ii) Zr has four predominantly s-process isotopes, ^{90}Zr, ^{91}Zr, ^{92}Zr, and ^{94}Zr, and one predominantly r-process isotope, ^{96}Zr; and (iii) because of the relatively long half-life of ^{95}Zr ($t_{1/2} \sim 64$ days), the production of ^{96}Zr by the s-process is a sensitive indicator of neutron density. Evidence for nucleosynthesis of Zr in red giant stars is provided by the observations of radioactive ^{93}Zr ($t_{1/2} \sim 1.5$ million years) in ZrO molecules of cool S-type stars (*26*–*29*). We have developed an instrument that combines a high-sensitivity, high-specificity mass spectrometer with micrometer-size sampling capability, and we report here measurements of Zr isotope ratios in individual SiC grains.

About 200 grains of the 3.4- to 5.9-μm size fraction (labeled "KJH") from the Murchison meteorite (*30*) were pressed into soft gold. Scanning electron microscopy with energy-dispersive x-ray microanalysis showed that about one-third of the grains in this mount were SiC; the remainder were hibonite and corundum. Isotopic analysis of Zr in presolar SiC is challenging, because of isobaric interferences from other elements and compounds. Zirconium has the following isobaric overlaps: Mo at masses 92, 94, and 96; Ru at mass 96; and Ti$_2$ at masses 92, 94, and 96 (with the most abundant mass peak of Ti$_2$ and the least abundant isotope of Zr at mass 96). Molybdenum is present in SiC (*31*), and Ru has been reported as grains (as either metal or a carbide) within presolar graphite spherules (*32*) and could be present in SiC. In addition, Ti is an abundant element in presolar SiC (*30*), and, hence, Ti$_2$ is a potential mass interference. The mass resolution needed to resolve these interferences, $M/\Delta M$ of 8×10^3 to 4×10^5, is beyond the capability of available secondary ion mass spectrometers. We developed an instrument, the Chicago-Argonne resonant ionization spectrometer for microanalysis (CHARISMA), that combines laser-induced thermal desorption of the sample with selective resonant photoionization of a specific element (for example, Zr) while leaving potential isobaric interferences (for example, Mo, Ru, and Ti$_2$) in the neutral state (*33*).

Thirty grains from KJH were ablated in CHARISMA, and 11 had Zr concentrations high enough to make isotopic measurements (*34*). In addition to the individual grains, we also analyzed an aggregate sample of the Murchison 0.32- to 0.70-μm grain-size separate (labeled "KJB") (*30*). It is common practice to normalize to the most abundant isotope when reporting isotope ratios. We have chosen instead to normalize our data to ^{92}Zr, because of a potential analytical artifact that could yield undercounting of the most abundant isotope, ^{90}Zr (*35*). Instrumental fractionation, primarily enhanced laser resonant ionization of ^{91}Zr (*34*), is corrected for by normalization to isotopic data collected on terrestrial samples. Results of the SiC analyses are reported in δ notation (*36*) (Table 1 and Figs. 1 and 2). All KJH SiC grains analyzed have large depletions in ^{96}Zr, small or no depletions in ^{90}Zr, small depletions or enrichments in ^{91}Zr, and small or no enrichments in ^{94}Zr, compared with a terrestrial composition standard. The isotopic pattern

---

G. K. Nicolussi, Enrico Fermi Institute, University of Chicago, Chicago, IL 60637, USA, and Chemistry and Materials Science Divisions, Argonne National Laboratory, Argonne, IL 60439, USA.
A. M. Davis, R. S. Lewis, S. Amari, Enrico Fermi Institute, University of Chicago, Chicago, IL 60637, USA.
M. J. Pellin, Chemistry and Materials Science Divisions, Argonne National Laboratory, Argonne, IL 60439, USA.
R. N. Clayton, Enrico Fermi Institute, Department of Chemistry, and Department of the Geophysical Sciences, University of Chicago, Chicago, IL 60637, USA.

*Present address: McDonnell Center for Space Sciences, Washington University, St. Louis, MO 63130, USA.

of the fine-grained KJB SiC aggregate plots among the individual KJH grains.

The isotopic compositions of heavy elements have previously been measured in aggregates of SiC grains. In those studies, the isotopic compositions generally appeared to be mixtures of two components, the first of near-solar isotopic composition and the second of essentially end-member s-process products. The data for Zr (Fig. 2) also appear to be the result of mixing of two such components, one of near solar Zr isotopic composition and the other strongly depleted in ^{96}Zr. The isotopic composition of individual grains does not vary as laser ablation proceeds, so the presence of two Zr isotopic components must reflect mixing before formation of the SiC grains.

Mainstream SiC grains are generally believed to have formed around TP-AGB stars (*13*). These stars have periodic pulses occurring tens of thousands of years apart that mix s-process nuclei produced deep in the star's interior into the outer portions (*37, 38*). During the interpulse period, these stars consist of a C–O core, a thin H-burning shell, and a convective H-rich envelope. As H burning proceeds, He builds up beneath the H-burning shell, the star contracts, the temperature increases, and neutrons are produced through ^{13}C(α,n) ^{16}O (where n stands for neutron). When the temperature and He abundance become high enough, He burning is explosively ignited, and the star develops a He-burning shell. The energy release from He burning causes the star to expand, H burning is temporarily inactivated, and the convective envelope penetrates into the top region of the He shell. In this so-called third dredge-up, s-process nuclei produced during the interpulse period are mixed into the envelope and some H can mix downward to make ^{13}C from ^{12}C. The He-burning flash may only last 150 years because He is exhausted, after which the star contracts and the H-burning shell is reactivated (*39*). Strong stellar winds can drive off material from the outer, cooler part of the H-rich envelope of the star, allowing condensation to occur in the circumstellar envelope. The H-rich convective envelope is generally considered to be similar in heavy-element isotopic composition to the solar system before s-process products from the He shell are dredged up. A TP-AGB star undergoes a series of thermal pulses, with increasing amounts of s-process products dredged up and mixed into the envelope. TP-AGB stars continually lose mass in the form of ejected gas and condensate dust. A particular SiC grain will condense during the long interval between thermal pulses and should be uniform in isotopic composition. Dust grains that condense after only a few pulses should have Zr isotopic compositions close to that of our solar system, whereas those that condense late in the history of a TP-AGB star should be highly enriched in s-process Zr. In our analyses, single SiC grains were partially ablated

Table 1. Zirconium isotopic compositions of an aggregate (agg.) of KJB SiC grains and of individual, KJH SiC grains from the Murchison meteorite, given as δ values (*36*) and normalized to ^{92}Zr. Uncertainties are ±2σ, and the upper limit for δ^{96}Zr in 111 is 2σ, based on counting statistics, and includes uncertainties in interference correction and instrumental discrimination. Terrestrial Zr consists of 51.45% ^{90}Zr, 11.22% ^{91}Zr, 17.15% ^{92}Zr, 17.38% ^{94}Zr, and 2.80% ^{96}Zr.

Grain	Size (μm)	δ^{90}Zr (per mil)	δ^{91}Zr (per mil)	δ^{94}Zr (per mil)	δ^{96}Zr (per mil)
KJB agg.		−44 ± 66	−47 ± 89	118 ± 92	−922 ± 234
9	7.5	−130 ± 54	110 ± 90	39 ± 76	−934 ± 79
14	3	11 ± 151	−51 ± 94	55 ± 95	−615 ± 90
22	4	−149 ± 60	−200 ± 68	105 ± 78	−983 ± 308
50	4	−8 ± 56	−65 ± 70	3 ± 70	−526 ± 100
54	3	−117 ± 83	−90 ± 114	40 ± 116	−432 ± 149
70	4	11 ± 64	32 ± 86	13 ± 76	−653 ± 97
102	4	10 ± 77	33 ± 102	8 ± 93	−580 ± 96
111	3.5	−42 ± 63	6 ± 88	78 ± 84	<−775
126	5	−101 ± 63	−142 ± 106	1 ± 112	−441 ± 143
151	4	−112 ± 62	−9 ± 59	44 ± 52	−755 ± 61
154	5.5	−155 ± 117	−90 ± 82	37 ± 86	−492 ± 94

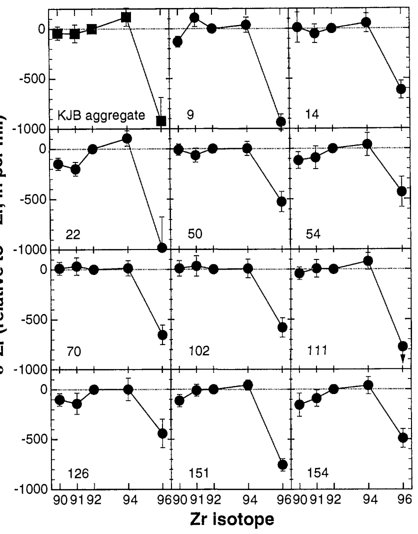

Fig. 1. Zirconium isotope patterns as a function of mass for single 3- to 8-μm SiC grains (circles) and an aggregate of 0.32- to 0.70-μm SiC grains (squares) from the Murchison meteorite, given as δ values relative to ^{92}Zr (*36*). For grain 111, a 2σ upper limit for δ^{96}Zr is indicated by an arrow.

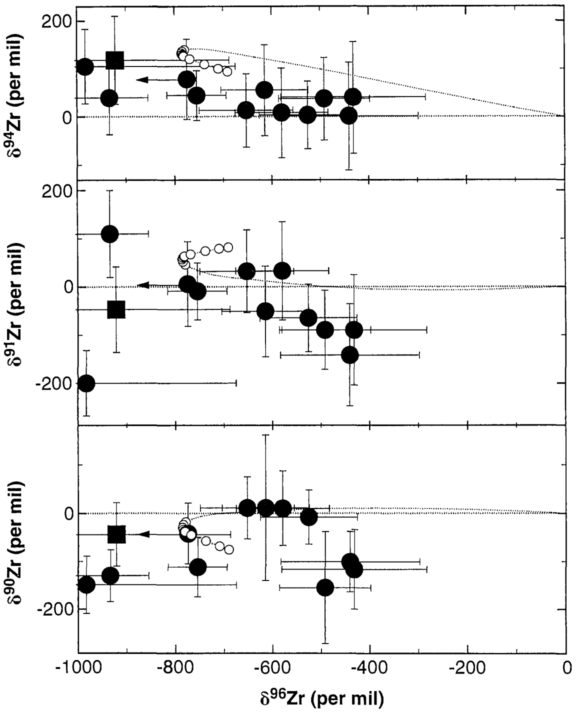

Fig. 2. Scatterplots of Zr δ values (*36*) for single 3- to 8-μm SiC grains (solid circles) and an aggregate of 0.32- to 0.70-μm SiC grains (solid squares) from the Murchison meteorite. Also shown are isotopic compositions of SiC grains predicted to condense from the envelope of a 1.5-$M_{\odot}$ (small open circles) AGB star after successive third dredge-up episodes (*42*). Symbols are only shown along this trajectory when the C/O ratio is >1. In earlier episodes, the C/O ratio of the envelope is too low to allow condensation of SiC. Other models with different stellar masses and neutron densities predict condensation of SiC with different ranges of δ^{96}Zr, but each model can only condense SiC with a narrow range of δ^{96}Zr. It is likely that the range of Zr isotopic data was produced in many TP-AGB stars with a range of masses and densities that condensed SiC grains with varying numbers of thermal pulses.

before Zr isotopic measurements were made. The Zr atoms analyzed are from the interiors of the SiC grains. The fact that individual grains show differing degrees of ^{96}Zr depletion relative to ^{92}Zr indicates mixing of s-process Zr with Zr of normal isotopic composition in the stars in which the grains formed and is the stars in which the grains formed and is consistent with the formation of these SiC grains around TP-AGB stars.

The primary source of neutrons for the s-process in TP-AGB stars is thought to be ^{13}C(α,n)^{16}O, where ^{13}C is produced by proton capture on ^{12}C during interpulse periods (*38–40*). This reaction produces fairly low neutron densities (about 10^7 cm^{-3}), so that most ^{95}Zr decays before it can capture another neutron to form ^{96}Zr (*41*). Any preexisting ^{96}Zr in the s-process region is transformed by neutron capture and beta decay to ^{97}Mo. A representative calculation (*42*) (Fig. 2) illustrates an evolutionary path for successive thermal pulses in a single AGB star of 1.5 $M_\odot$, for comparison with the measured compositions. For this mass and solar metallicity, the ^{13}C abundance was adjusted to fit C, Kr, Sr, Xe, and Ba isotopic abundances in the mainstream SiC grain population.

The calculation agrees with the observed Zr isotopic compositions of the grains, in the sense that large deficits in ^{96}Zr, small deficits in ^{90}Zr, and small excesses in ^{94}Zr are predicted and observed. Only for ^{91}Zr is a small excess predicted and a small deficit observed. Zirconium-90, ^{91}Zr, ^{92}Zr, and ^{94}Zr are produced and ^{96}Zr is consumed by the s-process. In the later thermal pulses of a TP-AGB star, the bottom of the convective shell may become hot enough to marginally activate the ^{22}Ne(α,n)^{25}Mg reaction, producing a short burst of high neutron density (10^8 to 10^{10} cm^{-3}). Under these conditions, 64-day ^{95}Zr may capture a neutron to form ^{96}Zr before beta decay occurs, causing the turnaround in the calculated trajectory (Fig. 2).

Condensation of SiC grains around the star from material ejected from the envelope requires that the ejecta have a C/O ratio > 1 (*43*). The C/O ratio increases with successive third dredge-up episodes. In Fig. 2, the symbols along the track appear only when the C/O ratio exceeds 1 and SiC can condense. A single TP-AGB star evolutionary model with a fixed mass, metallicity, and ^{13}C abundance cannot explain the range in Zr isotopic compositions of mainstream SiC grains. Other models with different stellar masses and neutron densities can explain portions of the data, but each model can only condense SiC with a narrow range of δ^{96}Zr. It is likely that the wide range of Zr isotopic data occurs because the SiC grains analyzed condensed around many TP-AGB stars with a range of masses and neutron densities.

REFERENCES AND NOTES

1. J. H. Reynolds and G. Turner, *J. Geophys. Res.* **69**, 3263 (1964).
2. D. C. Black, *Geochim. Cosmochim. Acta* **36**, 377 (1972).
3. R. N. Clayton, L. Grossman, T. K. Mayeda, *Science* **182**, 485 (1973).
4. R. S. Lewis, M. Tang, J. F. Wacker, E. Anders, E. Steel, *Nature* **326**, 160 (1987).
5. T. L. Daulton, D. D. Eisenhour, T. J. Bernatowicz, R. S. Lewis, P. R. Buseck, *Geochim. Cosmochim. Acta* **60**, 4853 (1996).
6. T. Bernatowicz *et al.*, *Nature* **330**, 728 (1987).
7. E. Zinner, M. Tang, E. Anders, *ibid.*, p. 730.
8. S. Amari, E. Anders, A. Virag, E. Zinner, *ibid.* **345**, 238 (1990).
9. I. D. Hutcheon, G. R. Huss, A. J. Fahey, G. J. Wasserburg, *Astrophys. J.* **425**, L97 (1994).
10. L. R. Nittler, C. M. O. Alexander, X. Gao, R. M. Walker, E. Zinner, *Nature* **370**, 443 (1994).
11. ———, *Astrophys. J.* **483**, 475 (1997).
12. L. R. Nittler *et al.*, *ibid.* **453**, L25 (1995).
13. E. Anders and E. Zinner, *Meteoritics* **28**, 490 (1993).
14. U. Ott, *Nature* **364**, 25 (1993).
15. P. Hoppe, S. Amari, E. Zinner, T. Ireland, R. S. Lewis, *Astrophys. J.* **430**, 870 (1994).
16. R. S. Lewis, S. Amari, E. Anders, *Nature* **348**, 293 (1990).
17. R. Gallino, M. Busso, G. Picchio, C. M. Raiteri, *ibid.*, p. 298.
18. E. M. Burbidge, G. R. Burbidge, W. A. Fowler, F. Hoyle, *Rev. Mod. Phys.* **29**, 547 (1957).
19. U. Ott and F. Begemann, *Lunar Planet. Sci.* **21**, 920 (1990).
20. E. Zinner, S. Amari, R. S. Lewis, *Astrophys. J.* **382**, L47 (1991).
21. S. Richter, U. Ott, F. Begemann, in *Nuclei in the Cosmos*, F. Käppeler and K. Wisshak, Eds. (Institute of Physics, Philadelphia, PA, 1992), pp. 127–132.
22. C. A. Prombo, F. A. Podosek, S. Amari, R. S. Lewis, *Astrophys. J.* **410**, 393 (1993).
23. R. S. Lewis, S. Amari, E. Anders, *Geochim. Cosmochim. Acta* **58**, 471 (1994).
24. S. Richter, U. Ott, F. Begemann, *Meteoritics* **29**, 522 (1994).
25. S. Amari, P. Hoppe, E. Zinner, R. S. Lewis, *ibid.* **30**, 679 (1995).
26. A. C. Zook, *Astrophys. J.* **221**, L113 (1978).
27. R. A. Malaney, in *Advances in Nuclear Astrophysics*, E. Vangioni-Flam *et al.*, Eds. (Editions Frontières, Gif-Sur-Yvette, France, 1986), pp. 407–417.
28. G. Wallerstein and J. F. Dominy, *Astrophys. J.* **330**, 937 (1988).
29. D. L. Lambert, V. V. Smith, M. Busso, R. Gallino, O. Straniero, *ibid.* **450**, 302 (1995).
30. S. Amari, R. S. Lewis, E. Anders, *Geochim. Cosmochim. Acta* **58**, 459 (1994).
31. G. K. Nicolussi *et al.*, *Lunar Planet. Sci.* **28**, 1021 (1997).
32. T. J. Bernatowicz *et al.*, *Astrophys. J.* **472**, 760 (1996).
33. Z. Ma, R. N. Thompson, K. R. Lykke, M. J. Pellin, A. M. Davis, *Rev. Sci. Instrum.* **66**, 3168 (1995).
34. The resonant laser radiation was generated by dye lasers pumped by a XeCl excimer laser. Laser-desorbed neutral Zr ground-state atoms from the SiC grains or terrestrial standards were ionized by this three-color scheme as follows: (i) 613.46-nm radiation excited Zr atoms resonantly from the $a^3F^\circ_2$ ground state to the intermediate $z^3F^\circ_2$ state; (ii) 472.39-nm radiation resonantly excited Zr atoms from this state to a higher intermediate state, e^3F_2; and (iii) 537.5-nm radiation ionized the excited Zr atoms through a resonant transition to just above the ionization limit (*44*). CHARISMA is equipped with an all-reflecting Schwarzschild-type optical microscope, which allows the sample to be viewed with ~1-μm spatial resolution and also permits introduction of a laser for ablation of the sample (*33*). The measurements were performed with a repetition rate of 20 Hz; each cycle consisted of the following sequence: (i) a 337-nm N_2 ablation laser pulse (pulse length ~3 ns), focused on a silicon carbide grain or standard, produced a cloud of neutral atoms, ions, and molecules; (ii) a voltage pulse was applied to an extraction electrode to electrostatically suppress the ions; (iii) the three resonant laser beams intersected the cloud of neutral species above the sample, resonantly ionizing Zr with high efficiency and nonresonantly ionizing other species with low efficiency; (iv) a positive 2000-V target pulse extracted and accelerated these photoions; (v) the photoions were mass- analyzed in a reflectron-type time-of-flight mass spectrometer with 4-m-long flight path; (vi) data were collected in an ion-counting mode, in which the signal produced by a single photoion was converted to a normalized voltage pulse (500 mV, 5 ns) and digitized in a 200-MHz transient recorder. Analysis of NIST Standard Reference Material (SRM) 1264a steel, which contains 690 ppm Zr, 4900 ppm Mo, and 2400 ppm Ti, showed no mass peaks of Mo and Ti_2 under Zr resonance ionization conditions. Zirconium metal and SRM 1264a were used as isotopic standards and are assumed to be of terrestrial isotopic composition. In addition, in each silicon carbide grain, a background mass spectrum was collected after two of the resonant lasers were detuned by 0.12 nm. In samples with nonresonant Ti in their mass spectra, a small peak at mass 96 from $^{48}Ti_2$ was seen. Resonant spectra were corrected for this interference, normalizing to the ^{48}Ti peak in both resonant and detuned spectra.
35. The ion-counting mode has the advantage that the signal-to-noise ratio is improved by reduction of electronic noise. A disadvantage may arise from systematic counting errors due to the limited time resolution of our detector system. The temporal distribution of photoions arriving at the detector (for one mass) has a full width at half maximum of ~30 ns. In some spectra, two (or more) photoion signals may fall within one 5-ns channel, and only one ion will be counted. Such an event is most likely if a large number of atoms are removed by the desorption laser. Because of pulse-to-pulse fluctuations of the desorption laser intensity, the amount of removed material per shot can vary significantly. To avoid significant counting errors, precise control of the incident laser intensity and very low average count rates (<1 count per channel per 100 shots) are necessary.
36. $\delta^{X}\mathrm{Zr} = [(^{X}\mathrm{Zr}/^{92}\mathrm{Zr})_{\mathrm{sample}}/(^{X}\mathrm{Zr}/^{92}\mathrm{Zr})_{\mathrm{standard}} - 1] \times 1000$; where X = 90, 91, 94, or 96 and the standard is NIST SRM 1264a.
37. I. Iben Jr. and A. Renzini, *Annu. Rev. Astron. Astrophys.* **21**, 271 (1983).
38. R. Gallino, C. Arlandini, M. Lugaro, M. Busso, O. Straniero, *Nucl. Phys. A*, in press.
39. R. Gallino, M. Busso, M. Lugaro, in *Astrophysical Implications of the Laboratory Study of Presolar Materials*, T. J. Bernatowicz and E. K. Zinner, Eds. (American Institute of Physics, New York, in press).
40. R. Gallino *et al.*, in preparation.
41. K. A. Toukan and F. Käppeler, *Astrophys. J.* **348**, 357 (1990).
42. R. Gallino, personal communication.
43. K. Lodders and B. Fegley Jr., *Meteoritics* **30**, 661 (1995).
44. D. R. Spiegel *et al.*, *Anal. Chem.* **66**, 2647 (1994).
45. We thank R. Gallino, C. Arlandini, M. Busso, M. Lugaro, O. Straniero, and C. Travaglia for discussions and for sharing the results of their models of nucleosynthesis in TP-AGB stars. Supported by NASA through grants NAGW-3342 (R.S.L.), NAGW-3345 (R.N.C.), and NAGW-3384 (A.M.D.) and by the U.S. Department of Energy, Basic Energy Sciences–Materials Sciences, under contract W-31-109-ENG-38.

1 April 1997; accepted 15 July 1997